USE OF EO-1 HYPERION DATA TO CALCULATE SPECTRAL BAND ADJUSTMENT FACTOR (SBAF) BETWEEN THE L7 ETM+ AND TERRA MODIS SENSORS

G. Chander[a], N. Mishra[b], D. L. Helder[b], D. Aaron[b], T. Choi[c], A. Angal[d], X. Xiong[e]

[a]SGT, Inc., U.S. Geological Survey (USGS) Earth Resources Observation and Science (EROS) Center, Sioux Falls, SD, 57198, USA. Work performed under U.S. Geological Survey contract 08HQCN0005
[b]South Dakota State University (SDSU), Brookings, SD, 57007, USA
[c]Sigma Space Corporation, 10210 Greenbelt Road, Lanham, MD, 20706, USA
[d]Science Systems and Applications (SSAI), Inc., 10210 Greenbelt Road, Lanham, MD, 20706, USA
[e]NASA Goddard Space Flight Center (GSFC), Greenbelt, MD, 20771, USA

1. INTRODUCTION

To monitor the land surface processes over a wide range of temporal and spatial scales, it is critical to have coordinated observations of the Earth's surface using imagery acquired from multiple spaceborne imaging sensors. However, an integrated global observation framework requires an understanding of how land surface processes are differently seen by various sensors. This is particularly true for the sensors acquiring data in spectral bands whose relative spectral responses (RSRs) are not similar and thus may produce significantly different results while observing the same target depending on the surface characteristics. The characterization and quantification of these effects are necessary to achieve an integrated Global Earth Observation System of Systems (GEOSS) for coordinated and sustained observation of the Earth.

Previous studies focused on monitoring the long-term on-orbit calibration stability of the Terra Moderate Resolution Imaging Spectroradiometer (MODIS) and the Landsat 7 (L7) Enhanced Thematic Mapper Plus (ETM+) sensors using the Committee on Earth Observation Satellites (CEOS) reference standard pseudo-invariant test sites (Libya 4, Mauritania 1/2, Algeria 3, Libya 1, and Algeria 5) [1], [2], & [3]. The ETM+ has six reflective spectral bands at 30 m spatial resolution with spectral coverage from 0.45 to 2.36 µm, one panchromatic band at 15 m spatial resolution, and one 60 m spatial resolution thermal band. The MODIS sensor has 36 spectral bands, with band center wavelengths ranging from 0.41 to 14.23 µm. MODIS Bands 1 and 2 have a spatial resolution of 250 m at nadir, Bands 3–7 of 500 m at nadir, and Bands 8–36 of 1 km at nadir.

In this study, a spectral band adjustment factor (SBAF) is derived using hyperspectral Earth Observing-1 (EO-1) Hyperion measurements. Hyperion is a high resolution grating imaging spectrometer, capable of resolving 220 spectral bands from 0.4 to 2.5 microns with 30 m spatial resolution, and provides near continuous (hyperspectral) information regarding the spectral signature of the ground. Hyperion images a 7.5 km by 100 km surface area and provides 10 nm (sampling interval) contiguous spectral bands. Fig. 1 illustrates a typical Libya 4 top-of-atmosphere (TOA) reflectance spectrum and compares the RSR profiles of the ETM+ and MODIS sensors.

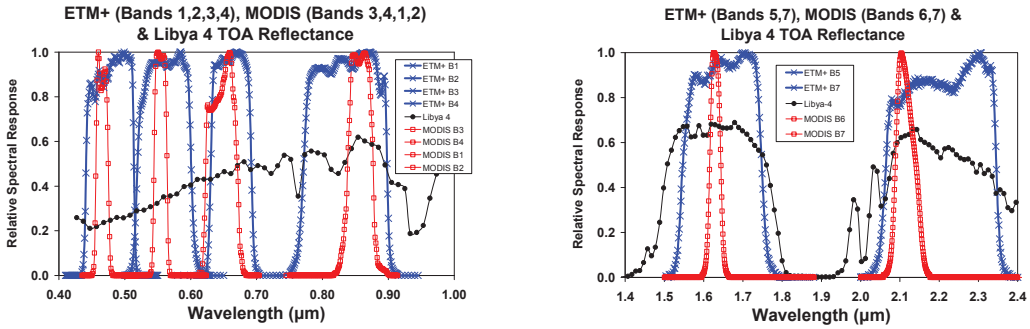

Fig. 1. Comparison of the Libya 4 TOA reflectance spectrum and the RSR profiles from the ETM+ and MODIS sensors.

The Libya 4 TOA reflectance spectrum was generated using an average of 19 cloud-free images from 2004 to 2009 acquired using the EO-1 Hyperion sensor. The SBAFs were calculated by convolving the spectral response of the ETM+ and MODIS sensors with the Hyperion TOA reflectance profile at each sampled wavelength, weighted by the respective RSR. To compensate the TOA reflectance data for sensor spectral response differences, the following equations [4], [5], & [6] were used.

$$\overline{\rho_\lambda} = \frac{\int \rho_\lambda \, RSR_\lambda d\lambda}{\int RSR_\lambda d\lambda} \tag{1}$$

$$SBAF = \frac{\rho_{ETM+}}{\rho_{MODIS}} = \frac{\left(\int \rho_\lambda \, RSR_{\lambda(ETM+)} d\lambda\right) / \left(\int RSR_{\lambda(ETM+)} d\lambda\right)}{\left(\int \rho_\lambda \, RSR_{\lambda(MODIS)} d\lambda\right) / \left(\int RSR_{\lambda(MODIS)} d\lambda\right)} \tag{2}$$

Now, RSR compensated ETM+ TOA reflectance would be

$$\rho^*_{ETM+} = \frac{\rho_{ETM+}}{SBAF} \tag{3}$$

Where

RSR_λ = Relative spectral response of the sensor [unitless]

ρ_λ = Hyperspectral TOA reflectance profile generated using the EO-1 Hyperion images [unitless]

ρ_{ETM+} = Band average TOA reflectance measurements generated using the ETM+ images [unitless]

ρ_{MODIS} = Band average TOA reflectance measurements generated using the MODIS images [unitless]

ρ^*_{ETM+} = RSR compensated Band average TOA reflectance measurements generated by dividing the lifetime ETM+ TOA reflectance with the band-specific SBAF values [unitless]

The Hyperion spectral resolution is on the order of 10 nm, and the spectral sampling intervals of the RSR are on the order of 2–3 nm. The Hyperion spectra are first resampled at a finer resolution to match the spectral interval of other sensors; otherwise, an error may be introduced in the estimation of SBAF. A quadratic interpolation was performed here, but some residual quantization error will remain that may affect the SBAF calculations. Once the band-specific SBAFs were calculated, the lifetime TOA reflectance measurements were compensated for the

spectral band differences. In this study, the lifetime ETM+ TOA reflectance were divided with the band-specific SBAF numbers to compensate for the RSR differences between the ETM+ and MODIS sensors. However, on the other hand similar RSR compensation could be done for the MODIS TOA reflectance measurements as well. In such a case same procedure can be repeated but now the band-specific SBAFs should be multiplied with their respective MODIS TOA reflectance measurements.

2. RESULTS AND DISCUSSION

The key data processing steps include: reprojection of MODIS Level 1B (L1B) data products, exclusion of scan-line corrector (SLC) fill values and images that are contaminated due to clouds, selection of a homogeneous region of interest (ROI), and conversion of calibrated digital numbers to TOA reflectance for the spectrally matching band pairs. Fig. 2 shows the long-term TOA reflectance trending of the spectrally matching bands of the ETM+ and MODIS sensors over the Libya 4 site. The measured TOA reflectances from MODIS (red squares) and ETM+ (blue crosses) have been trended for the Libya 4 site. A set of linear regressions were fitted to the TOA reflectance data. In general, the TOA reflectance linear regression fits for both sensors are observed to be parallel to each other. Thus there is showing a consistent long-term trend with small slopes and constant offsets. These constant offsets between the two sensors are most likely caused by a combination of the spectral signature of the ground target, atmospheric composition, and the RSR characteristics of each sensor.

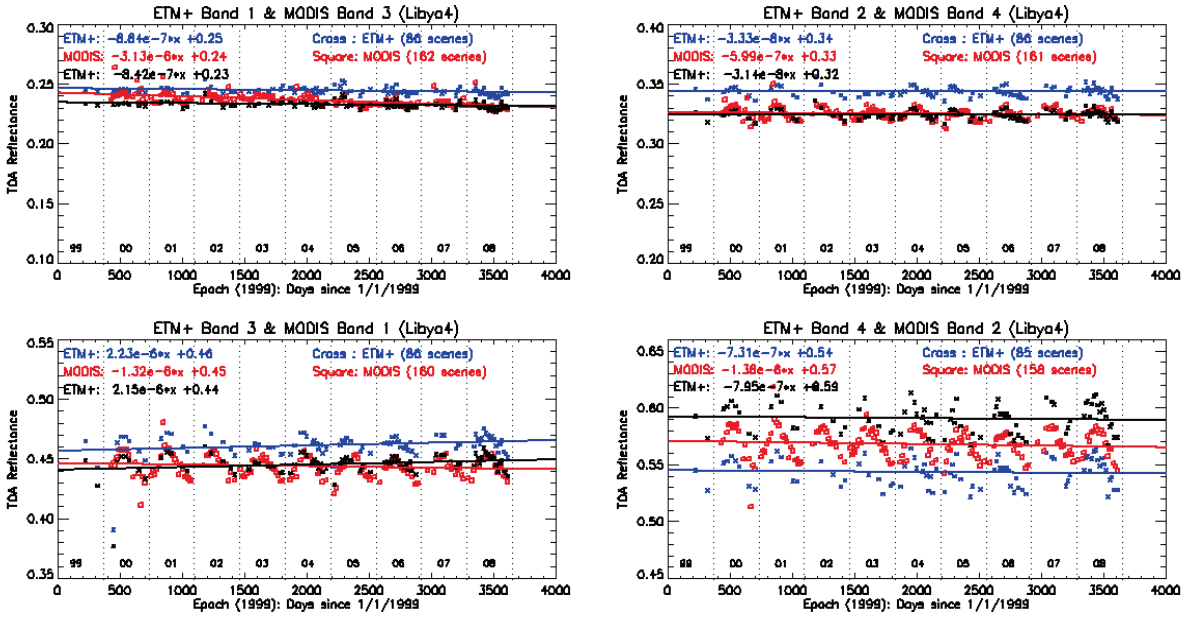

Fig. 2. TOA reflectance trending over the Libya 4 site.

The TOA reflectance profile obtained from EO-1 Hyperion is used as a representative of the surface reflectance of the ground target as passed upward through the atmosphere. In this study, EO-1 Hyperion–derived SBAFs were used to compensate for offset differences observed in the long-term trends. The SBAF-compensated ETM+ reflectances (black squares) are shown in the same figure. After spectral correction, the RSR compensated ETM+ TOA reflectance measurements show better agreement with MODIS. The agreement is better in the visible bands than the shortwave infrared bands. For Bands 1–3, the RSR compensated ETM+ TOA reflectances overlie the corresponding MODIS TOA reflectances. However, there seems to be an overcorrection for Band 4 and an undercorrection for Bands 5–7. The overcorrection for Band 4 is attributed to the presence of a water vapor absorption feature in ETM+, and the undercorrection for Bands 5–7 may be due to the lower agreement in the SWIR RSR between ETM+ and MODIS. The remaining uncertainty between the offsets can be attributed to different geometric registration, Bidirectional Reflectance Distribution Function (BRDF), atmospheric effects, and potential calibration differences between the sensors**.** Although the formulation of the SBAF and its application to a sample dataset are presented here, an in-depth study using additional hyperspectral images will be performed for future improvements.

3. REFERENCES

[1] G. Chander, A. Angal, T. Choi, D.J. Meyer, X. Xiong, and P.M. Teillet, "Cross-calibration of the Terra MODIS, Landsat-7 ETM+ and EO-1 ALI sensors using near simultaneous surface observation over Railroad Valley Playa, Nevada test site," in Proc. SPIE Int. Symp., Vol 6677, 6677-34, San Diego, CA, 2007.

[2] G. Chander, X. Xiong, X., T. Choi, and A. Angal, "Monitoring On-orbit radiometric stability of the Terra MODIS and Landsat 7 ETM+ sensors using pseudo-invariant test sites," *Remote Sensing of Environment*. (Accepted)

[3] G. Chander, J.B. Christopherson, G. L. Stensaas, and P. M. Teillet, "Online Catalogue of Worldwide Test Sites for the Post-Launch Characterization and Calibration of Optical Sensors," International Astronautical Federation - 58th International Astronautical Congress 3, pp. 2043-2051, Hyderabad, India, Sep. 24-28, 2007.

[3] C. Cao, X. Xiong, A. Wu, and X. Wu, "Assessing the consistency of AVHRR and MODIS L1B reflectance for generating Fundamental Climate Data Records," *J. Geophys. Res.*, 113, D09114, doi:10.1029/2007JD009363, 2008.

[4] C.J. Bruegge, N.L. Chrien, R.R. Ando, D.J. Diner, W.A. Abdou, M.C. Helmlinger, S.H. Pilorsz, K.J. Thome, and K.J. Early, "Validation of the Multi-angle Imaging Spectroradiometer (MISR) radiometric scale," *IEEE Trans. On Geosciences and Remote Sensing*, 40, pp. 1477–1492, 2002.

[6] P.M. Teillet, G. Fedosejevs, K.J. Thome, and J.L. Barker, "Impacts of spectral band difference effects on radiometric cross-calibration between satellite sensors in the solar-reflective spectral domain," *Remote Sensing of Environment*, 110, pp. 393–409, 2007.